NMF - Based Analysis of Droplet Wall-Film Interactions

Daniel Klötzl* and Daniel Weiskopf
Visualization Research Center (VISUS), University of Stuttgart, Stuttgart, Germany
*Corresponding author: daniel.kloetzl@visus.uni-stuttgart.de

Keywords
Nonnegative Matrix Factorization, Droplet Wall-Film Interactions, Visualization

Introduction

The automated and explainable characterization of droplet wall-film impact outcomes and secondary phenomena is of great interest to many modern technological applications and natural processes. We use nonnegative matrix factorization (NMF) to decompose ensembles of experiments of droplets impacting a thin liquid layer. In prior work, nonnegative matrix factorization was used to identify areas of interest in mobile eye-tracking recordings in an unsupervised way [1]. Here, a general approach to applying NMF for the analysis of multiple video data together with suitable visualization techniques is introduced that utilize the interpretable NMF decomposition (via their matrix dimensions):

$$\mathbf{X} \simeq \mathbf{WH}, \quad \mathbf{X} \in \mathbb{R}^{🌐 \times ⏱}, \mathbf{W} \in \mathbb{R}^{🌐 \times k}, \mathbf{H} \in \mathbb{R}^{k \times ⏱}.$$

In fact, NMF decomposes the data into user-defined $\boldsymbol{k}$ spatiotemporal components representing different phenomena throughout the recordings. As a result, each component offers a spatial representation and a temporal indicator that shows the occurrence within the recordings. The number of NMF components enables the user to either decompose the recordings into large-scale phenomena (low k) or small-scale outliers (high k).
We demonstrate the usefulness of our visual analysis with a challenging ensemble of monochrome camera recordings for different fluids, droplet sizes, zoom, and illumination.

Investigated dataset: The droplet splash dataset by Geppert [2] is given as an ensemble of monochrome camera images of a single droplet impacting a thin liquid layer. The experiments include different liquids for both droplets and wall-films and differ in impact velocities and droplet sizes, leading to different impact outcomes and secondary phenomena, see Figure 1 for exemplary frames of the droplet wall-film interaction experiment monochrome camera images. The former analysis of the droplet splash dataset consisted of manually constructing the regime map of the parameter space of an ensemble of fluids by an expert [3].

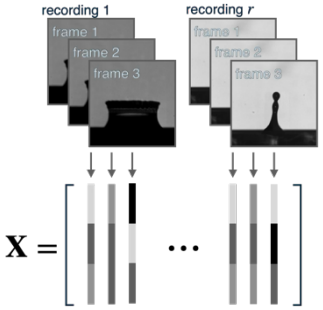

Figure 1. Stacking of recording frames to construct $\mathbf{X}$.

Goals and methods: The droplet splash recordings were performed in a more controlled, static setting compared to the mobile eye-tracking data. This study aims to introduce nonnegative matrix factorization to the analysis of droplet wall-film interaction. The NMF-based approach enables an exploratory analysis of multiple experiment recordings. Due to the natural interpretability of NMF, the usage is twofold: (1) for the identification of secondary phenomena, e.g., jet or bubble, and (2) to automatically differentiate impact velocities, fluids, and droplet sizes for multiple experiment recordings. This analysis of the crown shape and temporal evolution is of great interest [4]. Finally, we demonstrate the limitations and usefulness of our approach with different numbers of analyzed recordings and NMF-components $k \in \mathbb{N}$.

Methods and Dataset

For the visual analysis, NMF, introduced by Paatero and Tapper [5], is used to decompose the input data $\mathbf{X}$ into the interpretable factors $\mathbf{W}$ and $\mathbf{H}$ for $k \in \mathbb{N}$ (as denoted in the following).
For $k \in \mathbb{N}$ and $\mathbf{X} \geq 0$, $\min \|\mathbf{X} - \mathbf{WH}\|_{\text{fro}}$ with $\mathbf{W} \geq 0, \mathbf{H} \geq 0$, such that

$$\mathbf{X} = \begin{bmatrix} | & & | & & | & & | \\ x_1^{(1)} & \cdots & x_{m_1}^{(1)} & \cdots & x_1^{(r)} & \cdots & x_{m_r}^{(r)} \\ | & & | & & | & & | \end{bmatrix} \simeq \mathbf{WH}$$

$$= \begin{bmatrix} | & & | \\ w_1 & \cdots & w_k \\ | & & | \end{bmatrix} \cdot \begin{bmatrix} h_{1,1}^{(1)} & \cdots & h_{1,t_1}^{(1)} & \cdots & h_{1,1}^{(r)} & \cdots & h_{1,t_r}^{(r)} \\ \vdots & & \vdots & & \vdots & & \vdots \\ h_{k,1}^{(1)} & \cdots & h_{k,t_1}^{(1)} & \cdots & h_{k,1}^{(r)} & \cdots & h_{k,t_r}^{(r)} \end{bmatrix}.$$

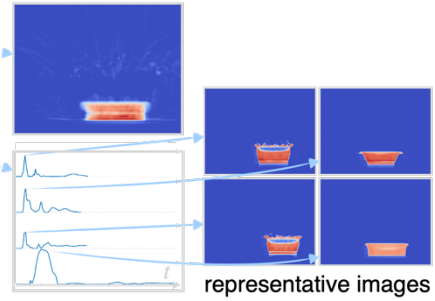

spatial components temporal components representative images

This decomposition leads to pairs of spatiotemporal components (w_j, h_j) for each NMF component $j \in \{1, \ldots, k\}$. As a result, each spatial component w_j can be embedded back into the image domain and the associated temporal component h_j (consisting of queued temporal components for each recording) is split into multiple vertically

arranged line charts, denoted as temporal indicator plots. These plots directly indicate the most relevant frames for each recording, expressed and highlighted as the respective representative images from the recordings. All computations follow Berry et al. [6] and were performed in MATLAB.

The droplet splash dataset consists of a total of 1300 recordings of droplet wall-film interactions. It contains experiments with different droplet diameters (2.2 mm to 4.0 mm), droplet velocities (0.1 m/s to 5.0 m/s), and film thicknesses (0.1 mm to 1.3 mm). The liquids used for the droplet and wall-film include, among others, hexadecane (hexa), hyspin, water, diesel, and engine oil. For the vectorization, every 10-th frame is used to reduce the total runtime. The monochrome frames of each recording are stacked consecutively to be further processed with NMF, as illustrated in Figure 1.

Results and Discussion

The proposed NMF-based analysis was performed for different settings and configurations using the vast droplet splash dataset by Geppert [2]. For the scope of this work, we restrict the detailed analysis to the following two controlled sets of recordings: 50 hyspin-hexa droplet wall-film interactions and the broader analysis of 12 preprocessed recordings with different droplet-wall fluid combinations.

Analysis of hyspin–hexadecane interaction. For the initial analysis, 50 hyspin-hexa droplet wall-film interactions are decomposed into six spatiotemporal components (only the first 12 recordings are illustrated in Figure 2). The NMF decomposition enables the distinction between the background (component 6) and different temporal components, e.g., crown formation (component 2), crown detachment (component 4), and splashing (components 1 and 5). As a first step, this characterization can be directly stated through the different spatial representations that hint at specific phenomena, e.g., the crown detachment in component 4. Furthermore, taking the temporal indicator plots into account, the temporal occurrence of the phenomena can be taken into perspective, e.g., the splashing (component 5) that is present throughout the rest of recordings 3 to 12 but stops early in recordings 1 and 2. Finally, the representative images show the specific maxima for each indicator plot and confirm the characterization, see component 2. Specifically, components 1, 4, and 6 show misleading results for the thin wall film (either being red or white). Filtering the recordings by subtracting the first frame leads to more comprehensible results, as the second analysis shows.

Analysis of droplet wall-film interactions for different fluids. For the second analysis, the investigated experiments are broadened to reflect different behaviors after the droplet impact, e.g., secondary phenomena. The investigated droplet wall-film combinations include hyspin-hexa (0.27, 0.23, 0.24, 0.25), diesel-engine oil (0.26, 0.74), hyspin-hyspin (0.26, 0.26), and hexa-hexa (0.25, 0.22, 0.51, 0.51), where the numbers in brackets denote the measured film thickness (in mm). Furthermore, the background noise is filtered out via subtraction of the respective first frame for each recording. As displayed in Figure 3, NMF successfully decomposes the dataset into different impact outcomes and secondary phenomena, e.g., the lamella (component 2) and resulting jet (component 5), as well as crown detachment (components 1, 4, and 6). Compared to the previous analysis, the filtering leads to more precise spatial representations and representative images. Furthermore, the temporal indicator plots show the temporal occurrence of the secondary phenomena and, therefore, enable the differentiation between impact velocities, fluids, and droplet sizes. This is specifically visible for component 5, where the indicator plots only show high impacts for

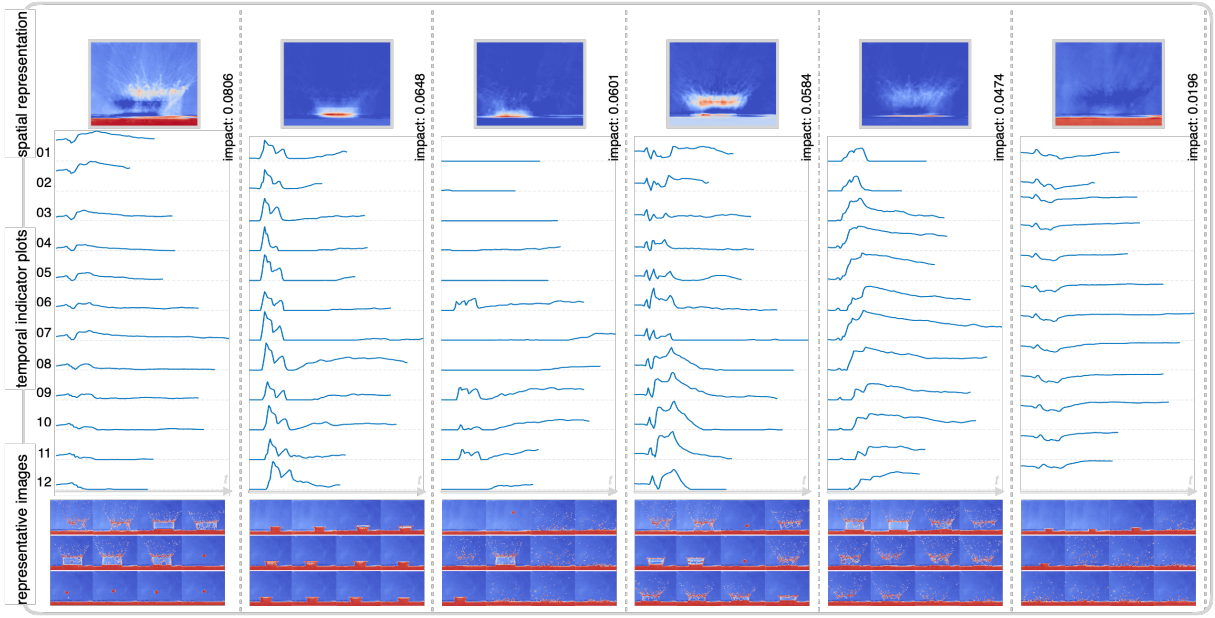

Figure 2. Application of our NMF-based visual analysis on 50 hyspin-hexa droplet wall-film interaction recordings. The data was decomposed into six spatiotemporal components and only the first 12 recordings are shown in the temporal indicator plots and representative images.

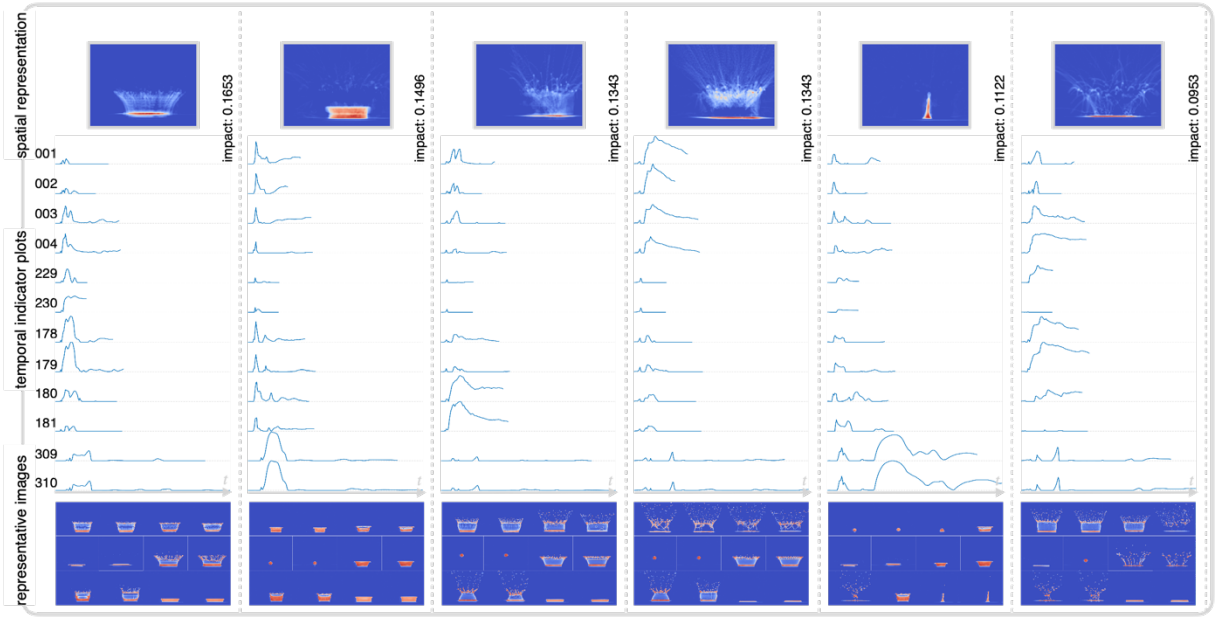

Figure 3. Application of our NMF-based visual analysis on 12 droplet wall-film interaction recordings with different droplet wall-film combinations, e.g., hyspin-hexa (0.27, 0.23, 0.24, 0.25), diesel-engine oil (0.26, 0.74), hyspin-hyspin (0.26, 0.26), and hexa-hexa (0.25, 0.22, 0.51, 0.51). The numbers in bracket denote the measured film thickness (in mm). The preprocessed data was decomposed into six spatiotemporal components.

recordings 309 and 310. Also, the lamella in component 2 is clearly visible and longer-lasting for these recordings. Again, the representative images confirm these observations. Very similar experiment configurations, e.g., recordings 180 and 181, as well as 229 and 230, also show similar temporal indicator plots in the NMF decomposition. In a similar analysis, we also included diesel-diesel droplet wall-film combinations. They are characterized via very long-lasting bubble formation as secondary phenomena. In the visual analysis, the resulting bubble wiped out all small-scale features in the spatial representations by arising for each of the components. Therefore, we excluded these experiments in the investigated set of configurations.

Discussion. To sum up, the extraction and distinction of different secondary phenomena is possible using the NMF-based analysis framework. This holds especially for the impact outcomes “jet” or “bubble.” The reduction of background noise, as well as a static viewpoint, is beneficial for the outcome of the analysis and should be included as a preprocessing step. To improve the decomposition even more, the recordings should be centered around the droplets for future studies. One goal of the study was to analyze multiple recordings simultaneously. While the study showed promising results for low recording numbers, the analysis with more than 200 recordings showed non-distinct results. Due to the broad information in the recordings, the spatial representations are mixed and specific impact outcomes and secondary phenomena are not isolated in the NMF components. Another limitation is the number of NMF components. If it is set too low, not enough features can be extracted, and for a high number of components ($k > 30$), specific frames were extracted, e.g., non-filtered background features or artifacts. One promising aspect for future work is the problem-specific (numerical) analysis of the temporal components ($-h_i -$). This could lead to better interpretability and comparability between specific recordings. Furthermore, similar components, identified via Wasserstein distance computation, could be clustered to reduce the number of spatiotemporal NMF components in post-processing.

Acknowledgments

This work was supported by the Deutsche Forschungsgemeinschaft (DFG, German Research Foundation) – Project-ID 270852890 – GRK 2160/2.

References

[1] D. Klötzl, T. Krake, F. Heyen, M. Becher, M. Koch, D. Weiskopf, and K. Kurzhals, “NMF-based analysis of mobile eye-tracking data,” in Proceedings of the Symposium on Eye Tracking Research and Applications, article no. 76, 2024.

[2] A. K. Geppert, “Experimental investigation of droplet wall-film interaction of binary systems,” Dissertation, University of Stuttgart, 2019.

[3] A. Geppert, A. Terzis, G. Lamanna, M. Marengo, and B. Weigand, “A benchmark study for the crown-type splashing dynamics of one- and two-component droplet wall-film interactions,” Experiments in Fluids 58, article no. 172, 2017.

[4] I. V. Roisman and C. Tropea, “Impact of a drop onto a wetted wall: description of crown formation and propagation,” Journal of Fluid Mechanics 472, 373–397, 2002.

[5] P. Paatero and U. Tapper. “Positive matrix factorization: A non-negative factor model with optimal utilization of error estimates of data values,” Environmetrics 5(2), 111–126, 1994.

[6] M. W. Berry, M. Browne, A.N. Langville, V. P. Pauca, and R. J. Plemmons, “Algorithms and applications for approximate nonnegative matrix factorization,” Computational Statistics and Data Analysis 52(1), 155–173, 2007.